Assessing flow alignment of nematic liquid crystals through linear viscoelasticity

L. R. P. de Andrade Lima and A. D. Rey*
Department of Chemical Engineering, McGill University, 3610 University Street, Montreal, Quebec, Canada H3A 2B2
(Received 29 October 2003; published 2 July 2004)

Shear alignment of rodlike nematic liquid crystals is found when the reactive parameter $\lambda > 1$. Measurements of λ usually require complex experiments. This paper presents a method based on the nematodynamic theory of Leslie and Ericksen that assesses flow alignment through small amplitude oscillatory flow. The method is based on the fact that the effect of λ on the storage modulus G' of linear viscoelasticity, when the director is along the flow direction, is directly proportional to $\lambda - 1$. Thus the alignment-nonalignment transition for increasing lambda is a reentrant viscoelastic transition: viscoelastic $(\lambda < 1) \rightarrow$purely viscous $(\lambda = 0) \rightarrow$viscoelastic $(\lambda > 1)$ that is reflected in the storage modulus G' and in the "loss angle" $\delta = \tan^{-1}(G''/G')$. The methodology is demonstrated by analyzing the Leslie-Ericksen equations for small-amplitude oscillatory Poiseuille flow of (4-n-octyl-4′-cyanobiphenyl) (8CB) using analytical and scaling methods. Since linear viscoelastic moduli are easily accessible, the proposed methodology is an additional useful and economical tool for nematodynamicists.

DOI: 10.1103/PhysRevE.70.011701 PACS number(s): 83.80.Xz, 83.60.Bc, 83.85.Cg, 47.50.+d

I. INTRODUCTION

Most liquid crystals exhibit polymorphism and are known to adopt different thermodynamic phases, typically increasing order as the temperature decreases. For instance, 4-n-octyl-4′-cyanobiphenyl (known as 8CB), which is a small molar mass thermotropic nematic liquid crystal (SMTNLC), adopts isotropic, nematic, smectic-*A* and solid phases as the temperature decreases under atmospheric pressure. The uniaxial nematic liquid crystalline phase has a long range one-dimensional orientational order but no positional order, whereas the smectics phase has, in addition to the orientational order, a one-dimensional positional order. The smectic-*A* phase is characterized by a layered structure that imparts a one-dimensional positional order, while the molecular orientation retains the order of the nematic liquid crystal phase. Thus the temperature changes of nematic flows lead to drastic changes in the rheological behavior [1,2].

A most significant temperature sensitive property is the shear flow aligning characteristics of uniaxial rodlike nematics, which is set by the sign and magnitude of the reactive order parameter λ; for the aligning regime $(\lambda > 1)$, the average molecular orientation or director **n**, is close to the streamline, while for the nonalignment regime $(0 \leqslant \lambda < 1)$, the steady state orientation is nonplanar and nonhomogeneous [3]. Some SMTNLC's such as 8CB exhibit flow-aligning behavior if the temperature is sufficiently high but at lower temperatures are nonaligning. At the flow aligning-nonaligning (*A-NA*) transition temperature $T_{a\text{-}na}$ the reactive parameter is equal to 1. Nonalignment is also observed in lyotropic nematic polymers [4]; at low shear rates, these materials are usually nonaligning, while at high shear rates they are aligning.

Since the reactive parameter plays such a crucial role in nematodynamics, its experimental measurement as well as theoretical predictions has been the focus of many studies [1,2,4]. Under flow aligning conditions the reactive parameter can be determined by optical methods. More generally, it can be determined indirectly by viscosity measurements or using startup flow, as is described by Larson [5] (see p. 463); for a recent review on measurement of viscosities in nematics see Moscicki [6]. When one wishes to ascertain whether a nematic liquid crystal is flow aligning or not, these optical and rheological experimental methods can be substituted by measuring the viscoelastic response to small-amplitude oscillatory shear flow, as shown in this paper where we propose an alternative and simpler rheological technique based on the linear viscoelastic theory and a standard oscillatory flow. Small amplitude oscillatory flows (SAOF's) are a main rheological tool used to characterize viscoelasticity [7,8] in terms of the storage $G'(\omega, T)$ and loss $G''(\omega, T)$ moduli as a function of frequency (ω) and temperature (T). Although simple shear is commonly used, pressure driven flows, as considered in this paper, are also equally useful [9,10]. Previous work on small-amplitude oscillatory shear of liquid crystals in a parallel plate geometry has been presented for rodlike nematic liquid crystals [11], nematic liquid crystal mixtures [12], chiral nematic liquid crystal [13], and side-chain nematic polymers [14]. In these theoretical studies the objective was to determine the relation between viscoelastic moduli and the material properties, such as the Frank elastic constants, the Miesowicz viscosities, and the rotational viscosity. In most of these theoretical studies it was found that monodomain nematic liquid crystals are viscoelastic in a frequency region surrounding the director relaxation time, and that the response in the small frequency terminal region corresponds to pure viscous material. Obviously, introduction of stable defect lattices would predict elastic response in the terminal zone, as observed by Ramos *et al.* [15] and by Yada *et al.* [16] for cholesteric liquid crystals. In this paper we show that the relatively simple SAOF measurements are also a useful tool to determine flow alignment in liquid crystals.

The objectives of this paper are:

*Corresponding author. Email address: alejandro.rey@mcgill.ca

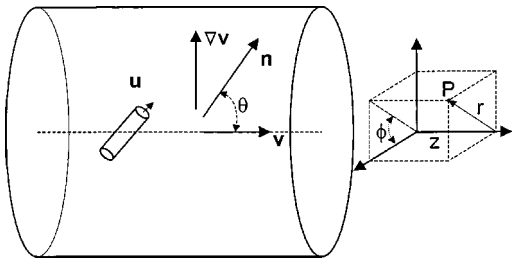

FIG. 1. Capillary flow of a uniaxial rodlike nematic liquid crystal, showing the unit normal vector (**u**), the director vector (**n**), the velocity vector (**v**), the velocity gradient ($\nabla\mathbf{v}$), the alignment angle (θ), and the cylindrical (r,ϕ,z) coordinate system used to describe a generic point P. Under pressure drop oscillation, the director vector fluctuates around $\mathbf{n}_o=(0,0,1)$.

(i) Characterize the temperature dependence of small amplitude oscillatory capillary Poiseuille flow (SAOPF) of nematic liquid crystals exhibiting an aligning-nonaligning transition.

(ii) Find the signatures of the aligning-nonaligning transition on the linear viscoelasticity of nematic liquid crystals.

(iii) Demonstrate the applicability of the small amplitude oscillatory capillary Poiseuille flow to characterize the alignment behavior of nematic liquid crystals, using 8CB as a model system.

This paper is organized as follows. Section II presents the governing equations and auxiliary data to describe the nematic liquid crystals oscillatory capillary Poiseuille flow. Section III presents the material viscoelastic properties and functions used to characterize the oscillatory Poiseuille flow of nematic liquid crystals. Section IV presents a characterization of the thermal dependence of the small amplitude oscillatory Poseuille flow of nematic liquid crystals using 8CB. The correspondence between temperature and reactive parameter effects on the storage modulus is established. Section V presents the signatures of flow alignment on linear viscoleasticity. Section VI presents the conclusions.

II. THEORY AND GOVERNING EQUATIONS

The governing equations of the Ericksen and Leslie theory consist of the linear momentum balance, director torque balance, and constitutive equations for the stresses, viscous and elastic torques, that take into account external forces that distort the spatially uniform equilibrium configurations of liquid crystals [1,2,17–19]. The orientation is defined by the director **n** that is a unit vector collinear with the average molecular orientation direction. Uniaxial nematic liquid crystals (NLC's) are characterized by an average molecular orientation represented by the director vector **n**, as shown in Fig. 1. For incompressible, inertialess, isothermal conditions the linear momentum balance is

$$\mathbf{0}=\mathbf{f}+\nabla\cdot\boldsymbol{\tau}, \tag{1}$$

where **f** is the body force per unit volume, and $\boldsymbol{\tau}$ is the total stress tensor. The constitutive equation for the total stress tensor $\boldsymbol{\tau}$ is

$$\boldsymbol{\tau}=-p\mathbf{I}-\frac{\partial F_d}{\partial\nabla\mathbf{n}}\cdot\nabla\mathbf{n}^T+\alpha_1(\mathbf{nn}:\mathbf{A})\mathbf{nn}+\alpha_2\mathbf{nN}+\alpha_3\mathbf{Nn}+\alpha_4\mathbf{A}+\alpha_5\mathbf{nn}\cdot\mathbf{A}+\alpha_6\mathbf{A}\cdot\mathbf{nn}, \tag{2}$$

$$\mathbf{A}=(\nabla\mathbf{v}+\nabla\mathbf{v}^T)/2; \tag{3a}$$

$$\mathbf{N}=\dot{\mathbf{n}}-\mathbf{W}\cdot\mathbf{n}; \tag{3b}$$

$$\mathbf{W}=(\nabla\mathbf{v}-\nabla\mathbf{v}^T)/2, \tag{3c}$$

where p is the pressure, **I** is the unit tensor, $\alpha_{i,\ i=1,2,3,4,5,6}$, are the six Leslie viscosity coefficients, **A** is the rate of deformation tensor, **N** is the corotational derivative of the director, and **W** is the vorticity tensor. In this theory the elastic free energy density F_d is given by

$$F_d=\tfrac{1}{2}K_{11}(\nabla\cdot\mathbf{n})^2+\tfrac{1}{2}K_{22}(\mathbf{n}\cdot\nabla\times\mathbf{n})^2+\tfrac{1}{2}K_{33}|\mathbf{n}\times\nabla\times\mathbf{n}|^2, \tag{4}$$

where K_{11}, K_{22}, and K_{33} are the splay, twist, and bend Frank elastic constants. The director torque balance equation is given by the sum of viscous (Γ^v) and elastic (Γ^e) torques:

$$\boldsymbol{\Gamma}^e+\boldsymbol{\Gamma}^v=\mathbf{0} \tag{5}$$

$$\boldsymbol{\Gamma}^e=-\mathbf{n}\times\left(\frac{\partial F_d}{\partial\mathbf{n}}-\nabla\frac{\partial F_d}{\partial(\nabla\mathbf{n})^T}\right); \tag{6a}$$

$$\boldsymbol{\Gamma}^v=-\mathbf{n}\times(\gamma_1\mathbf{N}+\gamma_2\mathbf{A}\cdot\mathbf{n}), \tag{6b}$$

$$\gamma_1=\alpha_3-\alpha_2; \tag{7a}$$

$$\gamma_2=\alpha_6-\alpha_5=\alpha_3+\alpha_2; \tag{7b}$$

$$\lambda=-\frac{\gamma_2}{\gamma_1}=-\frac{\alpha_6-\alpha_5}{\alpha_3-\alpha_2}=-\frac{\alpha_3+\alpha_2}{\alpha_3-\alpha_2}, \tag{7c}$$

where γ_1 is the rotational viscosity, and γ_2 is the irrotational torque coefficient. Due to Eq. (7b) there are only five independent Leslie coefficients. In addition, four thermodynamic inequalities introduce further magnitude restrictions on these coefficients [1,2,19]. The reactive parameter is involved in nondissipative processes but it is given by a ratio of dissipative coefficients [1,2].

The inertial term in the linear momentum balance equation, Eq. (1), and the director inertia in Eq. (5) are both neglected; the former is due to the fact that the velocity field evolves much faster than the orientation field, so the velocity relaxation time is irrelevant with respect to the orientation relaxation time [2] and the latter is because it is insignificant in comparison with the retained viscous terms.

Consider a small-amplitude oscillatory Poiseuille capillary flow of a nematic liquid crystal, driven by pressure drop oscillations of infinitesimal amplitude, as shown in Fig. 1. The cylindrical coordinate system is also defined in Fig. 1. The flow is described by an axisymmetric oscillatory planar director field $[\mathbf{n}(r,t)=(\sin\theta(r,t),0,\cos\theta(r,t))]$, and a purely axial oscillatory velocity field $[\mathbf{v}(r,t)=(0,0,v(r,t))]$

with finite velocity gradient at the centerline. Linearizing around the axial direction (i.e., $\sin\theta \cong \theta$, $\cos\theta \cong 1$), the dimensionless governing equations for the director tilt angle $\theta(\tilde{r},\tilde{t})$ and the axial velocity $\tilde{v}(\tilde{r},\tilde{t})$ simplify to [20]

$$\tilde{\eta}_{\text{splay}}\frac{\partial\theta}{\partial\tilde{t}} = \frac{\partial}{\partial\tilde{r}}\left(\frac{1}{\tilde{r}}\frac{\partial}{\partial\tilde{r}}(\tilde{r}\theta)\right) + \frac{\tilde{\alpha}_3}{2\,\tilde{\eta}_1}E\tilde{r}, \tag{8a}$$

$$\frac{\partial\tilde{v}}{\partial\tilde{r}} = -\frac{E\,\tilde{r}}{2\tilde{\eta}_1} + \tilde{B}, \tag{8b}$$

$$\tilde{B} = -\frac{\tilde{\alpha}_3}{\tilde{\eta}_1}\frac{\partial\theta}{\partial\tilde{t}}, \tag{9a}$$

$$\tilde{\eta}_{\text{splay}} = \tilde{\gamma}_1 - \frac{\tilde{\alpha}_3{}^2}{\tilde{\eta}_1}, \tag{9b}$$

where $\tilde{\eta}_{\text{splay}}$ is the dimensionless splay viscosity, $\tilde{\alpha}_i$ are the dimensionless Leslie viscosities $(\tilde{\alpha}_i=\alpha_i/\langle\eta\rangle)$, $\langle\eta\rangle$ is the average Miesowicz viscosity [20], $E(\tilde{\omega}\tilde{t})=(R^3/K_{11})\times[-(\mathrm{d}p/\mathrm{d}z)(\tilde{\omega}\tilde{t})]$ is the ratio of viscous flow effects to long-range elasticity effects known as the Ericksen number, $\tilde{r}=r/R$ is the dimensionless radius, R is the capillary radius, $\tilde{t}=K_{11}t/(R^2\langle\eta\rangle)$ is the dimensionless time, $\tilde{v}=\langle\eta\rangle R\,v/K_{11}$ is the scaled axial velocity, $-\mathrm{d}p/\mathrm{d}z$ is the given small amplitude oscillatory pressure drop in the capillary per unit length, $\tilde{\omega}=\omega(R^2\langle\eta\rangle)/K_{11}$ is the dimensionless frequency, and $\tilde{B}$ is the dimensionless backflow [21].

The boundary conditions for the director orientation angle represent strong planar anchoring, $\theta(0,\tilde{t})=\theta(1,\tilde{t})=0$, and for the axial velocity the no slip condition at the bounding surface is used, $\tilde{v}(1,\tilde{t})=0$. The director oscillates around the velocity (z) direction, and the undistorted director field is $\mathbf{n}_o=(0,0,1)$.

For the small amplitude oscillatory capillary Poiseuille flow considered in this paper, the Ericksen number (i.e., dimensionless pressure drop) oscillates as follows:

$$E = E_0\sin\tilde{\omega}\tilde{t}, \tag{10}$$

where E_o is the infinitesimal dimensionless amplitude. Note that the frequency ω is scaled with the orientation time scale $\tau_o=(R^2\langle\eta\rangle)/K_{11}$ and the maximum elastic storage is expected for frequencies close to the reciprocal of this value.

III. MATERIAL PROPERTIES

The viscoelastic material properties needed to characterize the small amplitude oscillatory Poiseuille flow of NLC's aligned along the capillary axis include the Miesowicz viscosities η_1, the reactive parameter λ, the torque coefficient α_3, and the re-orientation viscosity η_{splay} [2,19].

The Miesowicz shear viscosities that characterize viscous anisotropy are measured in a steady simple shear flow between parallel plates with fixed director orientations along three characteristic orthogonal directions: $\eta_1=(\alpha_3+\alpha_4+\alpha_6)/2$ when the director is parallel to the velocity direction, $\eta_2=(-\alpha_2+\alpha_4+\alpha_5)/2$ when it is parallel to the velocity gradient, and $\eta_3=\alpha_4/2$ when it is parallel to the vorticity axis; the measured Miesowicz shear viscosities for aligning nematics usually follow the ordering

$$\eta_2 > \eta_3 > \eta_1. \tag{11}$$

In the present flow η_1 is the relevant steady shear viscosity, but the average of the three Miesowicz viscosities are used for scaling proposes.

The shear flow alignment of rodlike NLC's is governed by the magnitude of the reactive parameter $\lambda\,(T)$. According to Eq. (7c), $\lambda=f(\alpha_2,\alpha_3)$, and for rods the inequality $\alpha_2<0$ holds at all temperatures, but α_3 may change sign. For rodlike molecules, when $\lambda>1$ $(\alpha_3<0)$ the material is known as shear flow aligning, and the director aligns within the shear plane, at an angle θ_L, known as the flow-alignment Leslie angle, given by [19]

$$\theta_L = \frac{1}{2}\cos^{-1}\left(\frac{1}{\lambda}\right). \tag{12}$$

In a steady simple shear flow when the director is aligned along θ_L the viscous torques are zero. The Leslie angle can be measured using optical methods and the reactive parameter can be evaluated directly using Eq.(12); however, when $\lambda<1$ $(\alpha_3>0)$, nonaligning behavior arises and Eq. (12) does not hold.

When the director angle is in the plane of shear and close to zero the viscous torque Γ^v_ϕ around the azimuthal direction is

$$\Gamma^v_\phi = -\alpha_3\theta\dot{\gamma} = -\frac{\gamma_1}{2}(1-\lambda)\theta\dot{\gamma} = \alpha_2\frac{(1-\lambda)}{(1+\lambda)}\theta\dot{\gamma}, \tag{13}$$

where $\dot{\gamma}$ is the characteristic shear rate, and where we used the definitions Eqs. (7a) and (7c). In SAOPF the viscous torque is balanced by the elastic torque, and thus measuring the linear viscoelastic storage and loss moduli yields α_3. Since for SMRNLC's the Leslie coefficient α_2 is always negative, the sign of α_3 determines whether λ is greater or less than 1. Thus flow alignment can be determined using simple and purely mechanical measurements. At the *A-NA* transition, the viscous torque vanishes: $\Gamma^v_\phi=0$.

The director reorientation is a viscoelastic process, and the re-orientation viscosities associated with splay, twist, and bend deformations are defined by [2,21]

$$\eta_{\text{twist}} = \gamma_1; \tag{14a}$$

$$\eta_{\text{splay}} = \gamma_1 - \frac{\alpha_3{}^2}{\eta_1} = \gamma_1\left(1 - \frac{\gamma_1}{4\eta_1}(1-\lambda)^2\right); \tag{14b}$$

$$\eta_{\text{bend}} = \gamma_1 - \frac{\alpha_2{}^2}{\eta_2} = \gamma_1\left(1 - \frac{\gamma_1}{4\eta_2}(1+\lambda)^2\right). \tag{14c}$$

These viscosities are given by the rotational viscosity (γ_1) decreased by a factor introduced by the backflow effect. Backflow is re-orientation driven flow and is essentially the reverse effect to flow-induced orientation. The general expression for the re-orientation viscosities can be re-written as

TABLE I. Viscosity coefficients to 4-n-octyl-4′-cyanobiphenyl (8CB) [22,23].

Set	1	2	3	4[a]	5	6	7
T (°C)	34.00	35.00	37.00	38.36	39.00	40.00	40.50
Leslie viscosities coefficients (Pa s)							
α_1	0.6510	0.1342	0.0382	0.0196	0.0138	0.0078	0.0060
α_2	−0.0707	−0.0696	−0.0587	−0.0500	−0.0458	−0.0371	−0.0305
α_3	0.0404	0.0140	0.0031	0.0000	−0.0011	−0.0034	−0.0055
α_4	0.0582	0.0560	0.0520	0.0497	0.0488	0.0478	0.0474
α_5	0.0644	0.0529	0.0472	0.0415	0.0388	0.0339	0.0315
α_6	0.0341	−0.0026	−0.0084	−0.0085	−0.0082	−0.0067	−0.0046
Reactive parameter							
λ	0.2725	0.6639	0.9013	1.0000	1.0512	1.2042	1.4436
Dimensionless Leslie viscosities coefficients ($\tilde{\alpha}_i=\alpha_i/\langle\eta\rangle$)[b]							
$\tilde{\alpha}_1$	10.166	2.6671	0.8932	0.5067	0.3735	0.2291	0.1855
$\tilde{\alpha}_2$	−1.1044	−1.3832	−1.3725	−1.2925	−1.2395	−1.0896	−1.9428
$\tilde{\alpha}_3$	0.6309	0.2782	0.07249	0.0000	−0.02978	−0.09985	−0.1700
$\tilde{\alpha}_4$	0.9089	1.1130	1.2159	1.2848	1.3207	1.4038	1.4652
$\tilde{\alpha}_5$	1.0057	1.0513	1.1037	1.0728	1.0501	0.9956	0.9737
$\tilde{\alpha}_6$	0.5325	−0.05167	−0.1964	−0.2197	−0.2219	−0.1968	−0.1422
Dimensionless rotational viscosity and irrotational torque coefficient							
$\tilde{\gamma}_1$	1.7350	1.6615	1.4450	1.2925	1.2097	0.9897	0.7728
$\tilde{\gamma}_2$	−0.4732	−1.1050	−1.3001	−1.2925	−1.2693	−1.1894	−1.1128
Dimensionless Miesowicz viscosities							
$\tilde{\eta}_1$	1.0362	0.6698	0.5460	0.5325	0.5345	0.5536	0.5765
$\tilde{\eta}_2$	1.5094	1.7738	1.8461	1.8251	1.8051	1.7445	1.6909
$\tilde{\eta}_3$	0.4544	0.5565	0.6080	0.6424	0.6604	0.7019	0.7326
Dimensionless re-orientation viscosities							
$\tilde{\eta}_{\text{twist}}$	1.7350	1.6615	1.4450	1.2925	1.2097	0.9897	0.7728
$\tilde{\eta}_{\text{splay}}$	1.3509	1.5459	1.4354	1.2925	1.2081	0.9717	0.7226
$\tilde{\eta}_{\text{bend}}$	1.4713	1.6178	1.4422	1.2925	1.2092	0.9840	0.7557

[a]The Leslie viscosities coefficients and the temperature in this case are interpolated values.
[b]The average Miesowicz viscosity is defined as: $\langle\eta\rangle=(\eta_1+\eta_2+\eta_3)/3$.

$\eta_\alpha=\gamma_1-\zeta_i^2/\eta_i$, where η_i denotes the corresponding Miesowicz viscosity and ζ_i the corresponding torque coefficient. Since twist is the only mode that creates no backflow then $\eta_{\text{twist}}=\gamma_1$. For a bend distortion the backflow is normal to **n** and hence the torque coefficient is α_2, and the Miesowicz viscosity is η_2. On the other hand, for a splay distortion the backflow is parallel to **n** and hence the torque coefficient is α_3, and the Miesowicz viscosity is η_1. In the present flow the relevant re-orientation viscosity is $\eta_{\text{splay}}=\gamma_1-\alpha_3^2/\eta_1$. For a material like 8CB, the splay viscosity, twist and bend viscosities are identical at the *A-NA* transition.

In this paper we use the viscoelastic material parameters of 8CB, shown in Table I [22,23]. The temperature dependence of rheology of 8CB under transient and steady simple shear flows was presented by Han and Rey [3]. At a temperature $T=T_{a\text{-}na}=38.36$ °C the reactive parameter is $\lambda=1$ and $\alpha_3=0$. As mentioned previously in this section for temperatures above $T_{a\text{-}na}$, $\lambda>1$ and $\alpha_3<0$ and flow alignment is observed, while for temperatures below $T_{a\text{-}na}$, $\lambda<1$ and $\alpha_3>0$ and nonalignment is observed. In this paper we discuss results in terms of λ, instead of α_3, without loss of generality. The relation between α_3 and λ is [2]: $\alpha_3=-\alpha_2(1-\lambda)/(1+\lambda)$. Using Table I it can be seen that $d\lambda/d\alpha_3<0$ at all temperatures. Since for any function f, $\mathrm{df}/d\alpha_3=(\mathrm{df}/d\lambda)(d\lambda/d\alpha_3)$, it follows that $\mathrm{sgn}(\mathrm{df}/d\alpha_3)=-\mathrm{sgn}(\mathrm{df}/d\lambda)$ for all temperatures, and no ambiguities will arise.

IV. RESULTS AND DISCUSSION

The semicoupled set of equations, Eqs. (8a) and (8b), is solved by separation of variables. Note that the velocity partial time derivative is missing in Eq. (8b), and hence the velocity time dependence is set by the director dynamics. Symbolic and numerical calculations presented in the next

sections were performed using the software maple release 7 by Waterloo Maple Inc and matlab version 6.5 by MathWorks Inc.

A. Orientation field

Imposing pressure oscillations on the NLC's will produce spatially nonhomogeneous director oscillations. Since NLC's are viscoelastic the director oscillations will not be in phase with the applied pressure drop. Thus the total director angle $\theta(\tilde{r},\tilde{t},\tilde{\omega})$ is given by the sum of the following in-phase and out-phase components:

$$\theta(\tilde{r},\tilde{t},\tilde{\omega}) = \theta_i(\tilde{r},\tilde{\omega})\,\sin(\tilde{\omega}\tilde{t}) + \theta_o(\tilde{r},\tilde{\omega})\,\cos(\tilde{\omega}\tilde{t}). \quad (15)$$

Note that in phase means oscillation in phase with the imposed Ericksen number [see Eq. (10)], and hence the in-phase temporal variation is $\sin(\tilde{\omega}\tilde{t})$, while the out phase is $\cos(\tilde{\omega}\tilde{t})$. Using Eq. (8a) and separation of variables, the in-phase $\theta_i(\tilde{r},\tilde{\omega})$ and out-of-phase $\theta_o(\tilde{r},\tilde{\omega})$ director components are found to be

$$\theta_i = \frac{\tilde{\alpha}_3 E_0}{2\tilde{\eta}_1}\left(\frac{\mathrm{ber}_1\sqrt{\tilde{\omega}\tilde{\eta}_{\mathrm{splay}}}\tilde{r}\;\mathrm{bei}_1\sqrt{\tilde{\omega}\tilde{\eta}_{\mathrm{splay}}} - \mathrm{bei}_1\sqrt{\tilde{\omega}\tilde{\eta}_{\mathrm{splay}}}\tilde{r}\;\mathrm{ber}_1\sqrt{\tilde{\omega}\tilde{\eta}_{\mathrm{splay}}}}{\tilde{\omega}\tilde{\eta}_{\mathrm{splay}}\left(\mathrm{ber}_1{}^2\sqrt{\tilde{\omega}\tilde{\eta}_{\mathrm{splay}}} + \mathrm{bei}_1{}^2\sqrt{\tilde{\omega}\tilde{\eta}_{\mathrm{splay}}}\right)}\right), \quad (16)$$

$$\theta_o = \frac{\tilde{\alpha}_3 E_0}{2\tilde{\eta}_1}\left(\frac{\mathrm{ber}_1\sqrt{\tilde{\omega}\tilde{\eta}_{\mathrm{splay}}}\tilde{r}\;\mathrm{ber}_1\sqrt{\tilde{\omega}\tilde{\eta}_{\mathrm{splay}}} + \mathrm{bei}_1\sqrt{\tilde{\omega}\tilde{\eta}_{\mathrm{splay}}}\tilde{r}\;\mathrm{bei}_1\sqrt{\tilde{\omega}\tilde{\eta}_{\mathrm{splay}}}}{\tilde{\omega}\tilde{\eta}_{\mathrm{splay}}\left(\mathrm{ber}_1{}^2\sqrt{\tilde{\omega}\tilde{\eta}_{\mathrm{splay}}} + \mathrm{bei}_1{}^2\sqrt{\tilde{\omega}\tilde{\eta}_{\mathrm{splay}}}\right)} - \frac{\tilde{r}}{\tilde{\omega}\tilde{\eta}_{\mathrm{splay}}}\right), \quad (17)$$

where $\mathrm{bei}_\nu(x)$ and $\mathrm{ber}_\nu(x)$ are the Kelvin functions of order ν, [24]:

$$\mathrm{ber}_\nu(x) = \sum_{k=0}^{\infty} \frac{\cos\left(\frac{3\pi}{4}\nu + \frac{\pi}{2}k\right)}{k!\;\Gamma(k+1+\nu)}\left(\frac{x}{2}\right)^{2k+\nu}, \quad (18)$$

$$\mathrm{bei}_\nu(x) = \sum_{k=0}^{\infty} \frac{\sin\left(\frac{3\pi}{4}\nu + \frac{\pi}{2}k\right)}{k!\;\Gamma(k+1+\nu)}\left(\frac{x}{2}\right)^{2k+\nu}. \quad (19)$$

The amplitude of the director field θ is a function of $\tilde{\alpha}_3/\tilde{\eta}_{\mathrm{splay}}\tilde{\eta}_1$. The symmetry and scaling of the amplitudes are

$$\theta_i(\tilde{r},\tilde{\omega},\tilde{\alpha}_3) = -\,\theta_i(\tilde{r},\tilde{\omega},-\tilde{\alpha}_3), \quad \theta_o(\tilde{r},\tilde{\omega},\tilde{\alpha}_3) = -\,\theta_o(\tilde{r},\tilde{\omega},-\tilde{\alpha}_3), \quad (20)$$

$$\theta_i(\tilde{r},\tilde{\omega},\tilde{\alpha}_3) = \tilde{\alpha}_3 f_i(\tilde{r},\tilde{\omega}), \quad \theta_o(\tilde{r},\tilde{\omega},\tilde{\alpha}_3) = \tilde{\alpha}_3 f_o(\tilde{r},\tilde{\omega}). \quad (21)$$

Vanishing amplitudes are a signature of the aligment-nonalignment transition. The amplitude sign reversal indicates characteristic rheological responses. The only viscosities in the problem are the Miesowicz viscosity $\tilde{\eta}_1$ associated with the axially oriented director field [i.e. $\mathbf{n}=(0,0,1)$], and the transient splay viscosity $\tilde{\eta}_{\mathrm{splay}}$ associated with oscillations the director around the axial "z" axis. The frequency dependence of θ is weighted by the splay viscosity $\tilde{\eta}_{\mathrm{splay}}$ because the net flow effect on the director is renormalized by backflow.

Figure 2(a) shows the in phase component of the orientation (θ_i/E_o) as a function of the dimensionless radial distance $(\tilde{r})$ for dimensionless frequencies $(\tilde{\omega})$: 0.1, 1, 10, 100, 1000, and 10 000, $T=34\,^\circ\mathrm{C}$, and the reactive parameter 0.2725, in the nonaligning regime. Figure 2(b) shows the corresponding out-phase component of the orientation (θ_o/E_o) as a function of the dimensionless radial distance $(\tilde{r})$. The in-phase component decreases monotonically with frequency, while the out-of-phase component exhibits resonance behavior that signals maximum elastic storage. The behavior in the aligning regime is obtained by reversing the signs of the amplitudes.

B. Velocity field

Since the director field **n** is coupled to the velocity field **v**, imposing an oscillatory pressure drop to the NLC will produce a velocity field with in-phase and out-of-phase components. Thus the total dimensionless velocity field $\tilde{v}(\tilde{r},\tilde{t},\tilde{\omega})$ is given by the sum of the following in-phase and out-phase components:

$$\tilde{v}(\tilde{r},\tilde{t},\tilde{\omega}) = \tilde{v}_i(\tilde{r},\tilde{\omega})\,\sin(\tilde{\omega}\tilde{t}) + \tilde{v}_o(\tilde{r},\tilde{\omega})\,\cos(\tilde{\omega}\tilde{t}). \quad (22)$$

Using Eq. (8b) and separation of variables, the in-phase $\tilde{v}_i(\tilde{r},\tilde{\omega})$ and out-of-phase $\tilde{v}_o(\tilde{r},\tilde{\omega})$ director components are found to be

$$\tilde{v}_i=(1-\tilde{r}^2)\frac{E_0}{4\tilde{\eta}_1}\left(1+\frac{\tilde{\alpha}_3{}^2}{\tilde{\eta}_1\tilde{\eta}_{\text{splay}}}\right)+\frac{\tilde{\alpha}_3{}^2E_0}{2\tilde{\eta}_1{}^2\tilde{\eta}_{\text{splay}}}\left[\frac{\text{ber}_1\sqrt{\tilde{\omega}\tilde{\eta}_{\text{splay}}}(\text{ber}_0\sqrt{\tilde{\omega}\tilde{\eta}_{\text{splay}}}\tilde{r}-\text{bei}_0\sqrt{\tilde{\omega}\tilde{\eta}_{\text{splay}}}\tilde{r}-\text{ber}_0\sqrt{\tilde{\omega}\tilde{\eta}_{\text{splay}}}+\text{bei}_0\sqrt{\tilde{\omega}\tilde{\eta}_{\text{splay}}})}{\sqrt{2\tilde{\omega}\tilde{\eta}_{\text{splay}}}(\text{ber}_1{}^2\sqrt{\tilde{\omega}\tilde{\eta}_{\text{splay}}}+\text{bei}_1{}^2\sqrt{\tilde{\omega}\tilde{\eta}_{\text{splay}}})}\right]$$
$$+\frac{\tilde{\alpha}_3{}^2E_0}{2\tilde{\eta}_1{}^2\tilde{\eta}_{\text{splay}}}\left[\frac{\text{bei}_1\sqrt{\tilde{\omega}\tilde{\eta}_{\text{splay}}}(\text{bei}_0\sqrt{\tilde{\omega}\tilde{\eta}_{\text{splay}}}\tilde{r}+\text{ber}_0\sqrt{\tilde{\omega}\tilde{\eta}_{\text{splay}}}\tilde{r}-\text{bei}_0\sqrt{\tilde{\omega}\tilde{\eta}_{\text{splay}}}-\text{ber}_0\sqrt{\tilde{\omega}\tilde{\eta}_{\text{splay}}})}{\sqrt{2\tilde{\omega}\tilde{\eta}_{\text{splay}}}(\text{ber}_1{}^2\sqrt{\tilde{\omega}\tilde{\eta}_{\text{splay}}}+\text{bei}_1{}^2\sqrt{\tilde{\omega}\tilde{\eta}_{\text{splay}}})}\right], \tag{23}$$

$$\tilde{v}_o=-\frac{\tilde{\alpha}_3{}^2E_0}{2\tilde{\eta}_1{}^2\tilde{\eta}_{\text{splay}}}\left[\frac{\text{bei}_1\sqrt{\tilde{\omega}\tilde{\eta}_{\text{splay}}}(\text{ber}_0\sqrt{\tilde{\omega}\tilde{\eta}_{\text{splay}}}\tilde{r}-\text{bei}_0\sqrt{\tilde{\omega}\tilde{\eta}_{\text{splay}}}\tilde{r}-\text{ber}_0\sqrt{\tilde{\omega}\tilde{\eta}_{\text{splay}}}+\text{bei}_0\sqrt{\tilde{\omega}\tilde{\eta}_{\text{splay}}})}{\sqrt{2\tilde{\omega}\tilde{\eta}_{\text{splay}}}(\text{ber}_1{}^2\sqrt{\tilde{\omega}\tilde{\eta}_{\text{splay}}}+\text{bei}_1{}^2\sqrt{\tilde{\omega}\tilde{\eta}_{\text{splay}}})}\right]$$
$$+\frac{\tilde{\alpha}_3{}^2E_0}{2\tilde{\eta}_1{}^2\tilde{\eta}_{\text{splay}}}\left[\frac{\text{ber}_1\sqrt{\tilde{\omega}\tilde{\eta}_{\text{splay}}}(\text{bei}_0\sqrt{\tilde{\omega}\tilde{\eta}_{\text{splay}}}\tilde{r}+\text{ber}_0\sqrt{\tilde{\omega}\tilde{\eta}_{\text{splay}}}\tilde{r}-\text{bei}_0\sqrt{\tilde{\omega}\tilde{\eta}_{\text{splay}}}-\text{ber}_0\sqrt{\tilde{\omega}\tilde{\eta}_{\text{splay}}})}{\sqrt{2\tilde{\omega}\tilde{\eta}_{\text{splay}}}(\text{ber}_1{}^2\sqrt{\tilde{\omega}\tilde{\eta}_{\text{splay}}}+\text{bei}_1{}^2\sqrt{\tilde{\omega}\tilde{\eta}_{\text{splay}}})}\right]. \tag{24}$$

The in-phase component $\tilde{v}_i$ has a frequency-dependent term and a frequency-independent Newtonian parabolic component that is associated with the pure viscous contribution. The in-phase component $\tilde{v}_i$ is associated with the elastic contribution. The amplitude of the velocity field $\tilde{v}$ is a function of

$$R=\frac{-\tilde{\alpha}_3{}^2}{\tilde{\eta}_1^2\tilde{\eta}_{\text{splay}}}=\frac{(\tilde{\eta}_{\text{splay}}-\tilde{\gamma}_1)}{\tilde{\eta}_{\text{splay}}}\frac{1}{\tilde{\eta}_1}. \tag{25}$$

The transient viscosity information is contained in the dimensionless ratio $(\tilde{\eta}_{\text{splay}}-\tilde{\gamma}_1)/\tilde{\eta}_{\text{splay}}$ between net viscosity due to rotation and transient displacement viscosity. As usual $\tilde{\eta}_1$ is in the denominator and contains the steady "Newtonian" viscosity factor. The frequency dependence of $\tilde{v}$ is weighted by the splay viscosity $\tilde{\eta}_{\text{splay}}$ because the net flow effect is renormalized by backflow. The symmetry and scaling of the amplitudes are

$$v_i(\tilde{r},\tilde{\omega},\tilde{\alpha}_3)=v_i(\tilde{r},\tilde{\omega},-\tilde{\alpha}_3),\quad v_o(\tilde{r},\tilde{\omega},\tilde{\alpha}_3)=v_o(\tilde{r},\tilde{\omega},-\tilde{\alpha}_3), \tag{26}$$

$$v_i(\tilde{r},\tilde{\omega},\tilde{\alpha}_3)=(\tilde{\alpha}_3)^2g_i(\tilde{r},\tilde{\omega}),\quad v_o(\tilde{r},\tilde{\omega},\tilde{\alpha}_3)=(\tilde{\alpha}_3)^2g_o(\tilde{r},\tilde{\omega}). \tag{27}$$

Vanishing amplitudes are a signature of the alignment-nonalignment transition. The amplitudes are even functions of $\tilde{\alpha}_3$.

Figure 3(a) shows the in-phase dimensionless velocity component $(\tilde{v}_i/E_o)$ as a function of the dimensionless radial distance $(\tilde{r})$ for dimensionless frequencies $(\tilde{\omega})$: 0.1, 1, 10, 100, 1000, and 10 000, $T=34\,^\circ$C, and $\lambda=0.2725$, corresponding to the nonalignment regime. Figure 3(b) shows the corresponding out-phase dimensionless velocity component $(\tilde{v}_o/E_o)$ as a function of the dimensionless radial distance $(\tilde{r})$. As the frequency increases the profile of the in-phase component asymptotes the Newtonian parabola, while the out-phase component exhibits resonance. Identical behavior is observed in the aligning regime.

The out-phase velocity amplitude and the in-phase director amplitude exhibits boundary layer behavior that signals elastic storage. In steady simple shear flow the dimensionless director boundary layer thickness $\tilde{\xi}$ scales as $\tilde{\xi}\propto 1/\sqrt{E}$ [25]. Likewise in SAOPF the boundary layer thickness scales as $\tilde{\xi}\propto 1/\sqrt{\tilde{\omega}}$. By analyzing the dimensionless boundary layer thickness of the dimensionless out-phase velocity component as a function of the dimensionless frequency we find that the power law scaling holds for aligning and nonaligning regimes; at $T=T_{a\text{-}na}$, Newtonian viscous flow arises and $\tilde{v}_o\equiv 0$.

C. Viscoelastic material functions

The linear viscoelastic material functions are given by the complex modulus $\tilde{G}^*(\tilde{\omega})=\tilde{G}'(\tilde{\omega})+\text{iG}''(\tilde{\omega})$, where $\tilde{G}'$ is the dimensionless storage modulus and $\tilde{G}''$ is the dimensionless loss modulus. The dimensionless complex viscosity is defined by: $\tilde{\eta}^*(\tilde{\omega})=\tilde{\eta}'(\tilde{\omega})-i\tilde{\eta}''(\tilde{\omega})=\tilde{G}^*(\tilde{\omega})/\tilde{\omega}$, where $\tilde{\eta}'$ and $\tilde{\eta}''$ are the dissipative and elastic components. For Poiseuille flow the dimensionless flow rate $(\tilde{Q})$ and the dimensionless apparent viscosity $(\tilde{\eta})$ are given by the following relations [26]:

$$\tilde{Q}=2\pi\int_0^1\tilde{v}(\tilde{r})\tilde{r}d\tilde{r}, \tag{28a}$$

$$\tilde{\eta}=\frac{\pi E}{8\tilde{Q}}. \tag{28b}$$

Specifying these expressions for SAOPF using the dimensionless oscillatory flow rate given by

$$\tilde{Q}^*(\tilde{\omega},\tilde{t}) = \tilde{Q}_i(\tilde{\omega})\sin\tilde{\omega}\tilde{t} + \tilde{Q}_o(\tilde{\omega})\cos\tilde{\omega}\tilde{t}, \tag{29}$$

we obtain the following expressions for viscoleastic moduli:

$$\tilde{G}' = \frac{\pi E_0}{8}\frac{\tilde{Q}_o}{\tilde{Q}_i^2 + \tilde{Q}_o^2}\tilde{\omega}, \tag{30a}$$

$$\tilde{G}'' = \frac{\pi E_0}{8}\frac{\tilde{Q}_i}{\tilde{Q}_i^2 + \tilde{Q}_o^2}\tilde{\omega}. \tag{30b}$$

Using Eqs. (23), (24), and (28) the in-phase ($\tilde{Q}_i$) and out-of-phase ($\tilde{Q}_o$) flow-rate components are found to be

$$\tilde{Q}_i = \frac{\pi E_0}{8\tilde{\eta}_1}\left(1 + \frac{\tilde{\alpha}_3^2}{\tilde{\eta}_1\tilde{\eta}_{\text{splay}}}\right) + \frac{\pi E_0}{8\tilde{\eta}_1}\frac{8\tilde{\alpha}_3^2}{\tilde{\eta}_1\tilde{\eta}_{\text{splay}}}\left[\frac{\text{ber}_1\sqrt{\tilde{\omega}\tilde{\eta}_{\text{splay}}}\left(\frac{2}{\sqrt{2\tilde{\omega}\tilde{\eta}_{\text{splay}}}}\text{bei}_1\sqrt{\tilde{\omega}\tilde{\eta}_{\text{splay}}} + \frac{1}{2}\text{bei}_0\sqrt{\tilde{\omega}\tilde{\eta}_{\text{splay}}} - \frac{1}{2}\text{ber}_0\sqrt{\tilde{\omega}\tilde{\eta}_{\text{splay}}}\right)}{\sqrt{2\tilde{\omega}\tilde{\eta}_{\text{splay}}}(\text{ber}_1^2\sqrt{\tilde{\omega}\tilde{\eta}_{\text{splay}}} + \text{bei}_1^2\sqrt{\tilde{\omega}\tilde{\eta}_{\text{splay}}})}\right]$$
$$+ \frac{\pi E_0}{8\tilde{\eta}_1}\frac{8\tilde{\alpha}_3^2}{\tilde{\eta}_1\tilde{\eta}_{\text{splay}}}\left[\frac{\text{bei}_1\sqrt{\tilde{\omega}\tilde{\eta}_{\text{splay}}}\left(-\frac{2}{\sqrt{2\tilde{\omega}\tilde{\eta}_{\text{splay}}}}\text{ber}_1\sqrt{\tilde{\omega}\tilde{\eta}_{\text{splay}}} - \frac{1}{2}\text{bei}_0\sqrt{\tilde{\omega}\tilde{\eta}_{\text{splay}}} - \frac{1}{2}\text{ber}_0\sqrt{\tilde{\omega}\tilde{\eta}_{\text{splay}}}\right)}{\sqrt{2\tilde{\omega}\tilde{\eta}_{\text{splay}}}(\text{ber}_1^2\sqrt{\tilde{\omega}\tilde{\eta}_{\text{splay}}} + \text{bei}_1^2\sqrt{\tilde{\omega}\tilde{\eta}_{\text{splay}}})}\right], \tag{31}$$

$$\tilde{Q}_0 = \frac{\pi E_0}{8\tilde{\eta}_1}\frac{8\tilde{\alpha}_3^2}{\tilde{\eta}_1\tilde{\eta}_{\text{splay}}}\left[\frac{\text{bei}_1\sqrt{\tilde{\omega}\tilde{\eta}_{\text{splay}}}\left(-\frac{2}{\sqrt{2\tilde{\omega}\tilde{\eta}_{\text{splay}}}}\text{bei}_1\sqrt{\tilde{\omega}\tilde{\eta}_{\text{splay}}} - \frac{1}{2}\text{bei}_0\sqrt{\tilde{\omega}\tilde{\eta}_{\text{splay}}} + \frac{1}{2}\text{ber}_0\sqrt{\tilde{\omega}\tilde{\eta}_{\text{splay}}}\right)}{\sqrt{2\tilde{\omega}\tilde{\eta}_{\text{splay}}}(\text{ber}_1^2\sqrt{\tilde{\omega}\tilde{\eta}_{\text{splay}}} + \text{bei}_1^2\sqrt{\tilde{\omega}\tilde{\eta}_{\text{splay}}})}\right]$$
$$+ \frac{\pi E_0}{8\tilde{\eta}_1}\frac{8\tilde{\alpha}_3^2}{\tilde{\eta}_1\tilde{\eta}_{\text{splay}}}\left[\frac{\text{ber}_1\sqrt{\tilde{\omega}\tilde{\eta}_{\text{splay}}}\left(-\frac{2}{\sqrt{2\tilde{\omega}\tilde{\eta}_{\text{splay}}}}\text{ber}_1\sqrt{\tilde{\omega}\tilde{\eta}_{\text{splay}}} - \frac{1}{2}\text{bei}_0\sqrt{\tilde{\omega}\tilde{\eta}_{\text{splay}}} - \frac{1}{2}\text{ber}_0\sqrt{\tilde{\omega}\tilde{\eta}_{\text{splay}}}\right)}{\sqrt{2\tilde{\omega}\tilde{\eta}_{\text{splay}}}(\text{ber}_1^2\sqrt{\tilde{\omega}\tilde{\eta}_{\text{splay}}} + \text{bei}_1^2\sqrt{\tilde{\omega}\tilde{\eta}_{\text{splay}}})}\right]. \tag{32}$$

The frequency dependence of the viscoelastic moduli for $\tilde{\alpha}_3 \neq 0$ is as follows. The loss modulus is always greater than the storage modulus, the low frequency (terminal) regime is classic of a viscous fluid, and the characteristic slopes are

$$\text{as } \tilde{\omega} \to 0, \quad \tilde{G}' \sim \tilde{\omega}^2, \tilde{G}'' \sim \tilde{\omega};$$

$$\text{as } \tilde{\omega} \to \infty, \quad \tilde{G}' \sim \tilde{\omega}^{1/2}, \quad \tilde{G}'' \sim \tilde{\omega}. \tag{33}$$

The phase lag or "loss angle" $[\delta = \tan^{-1}(\tilde{G}''/\tilde{G}')]$ is characteristic of a viscoelastic material with a single relaxation time; in addition, the NLC is viscoelastic ($\delta < \pi/2$) at intermediate frequencies and purely viscous ($\delta = \pi/2$) at small and large frequencies.

Next we discuss the correspondence between $\tilde{G}' = \tilde{G}'(T,\tilde{\omega})$, $\tilde{G}'' = \tilde{G}''(T,\tilde{\omega})$ and $\tilde{G}' = \tilde{G}'(\lambda,\tilde{\omega})$, $\tilde{G}'' = \tilde{G}''(\lambda,\tilde{\omega})$. In other words, we wish to use the Leslie-Ericksen model to establish whether experimental measurements performed at different temperatures are good indicators of the magnitude of λ. Without loss of generality we discuss the results in terms of a normalized temperature T^*:

$$T^* = \lambda(T_1) + \left(\frac{T - T_1}{T_2 - T_1}\right)[\lambda(T_2) - \lambda(T_1)]. \tag{34}$$

We have checked that this scaled temperature T^* retains all the signatures found with the original temperature T scale. In particular, $\text{sgn}(d\tilde{G}'/\text{dT}) = \text{sgn}(d\tilde{G}'/\text{dT}^*)$.

Figure 4 shows the dimensionless loss modulus ($\tilde{G}''$) and the dimensionless storage modulus ($\tilde{G}'$) as a function of dimensionless frequency ($\tilde{\omega}$) for T(°C): 34, 35, 37, 38.36, 39, 40, and 40.5. By analyzing the dimensionless loss modulus as a function of the reactive parameter (λ) and scaled temperature (T^*) for given values of dimensionless frequency we find that this modulus is essentially independent of temperature and of λ:

$$\lambda < 1: \quad \frac{d\tilde{G}''(\tilde{\omega})}{d\lambda} \ll 1; \tag{35a}$$

$$\lambda > 1: \quad \frac{d\tilde{G}''(\tilde{\omega})}{d\lambda} \cong 0, \tag{35b}$$

$$T < 37\ ^\circ\text{C}: \quad \frac{d\tilde{G}''(\tilde{\omega})}{\text{dT}} \ll 1; \tag{35c}$$

$$T > 37\ ^\circ\text{C}: \quad \frac{d\tilde{G}''(\tilde{\omega})}{\text{dT}} \cong 0. \tag{35d}$$

This follows from the fact that the T and λ dependence of $\tilde{G}''$ is essentially through $\tilde{\eta}_1$, and according to Table I, for $T < 37\ ^\circ\text{C}$, $\tilde{\eta}_1$ is a very weak function of T; for $T > 37\ ^\circ\text{C}$, $\tilde{\eta}_1$ is essentially constant which explains the constant behav-

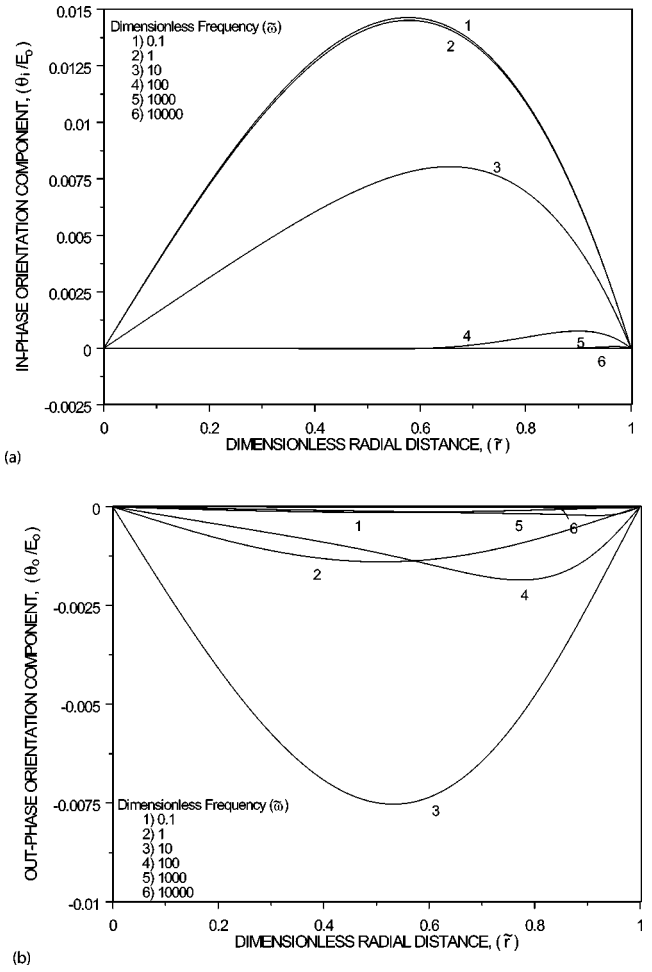

FIG. 2. Orientation components as a function of the dimensionless radial distance ($\tilde{r}$) for dimensionless frequencies ($\tilde{\omega}$): 0.1, 1, 10, 100, 1000, and 10 000, temperature 34 °C and reactive parameter 0.2725: (a) in-phase director component (θ_i/E_o); (b) out-phase director component (θ_o/E_o).

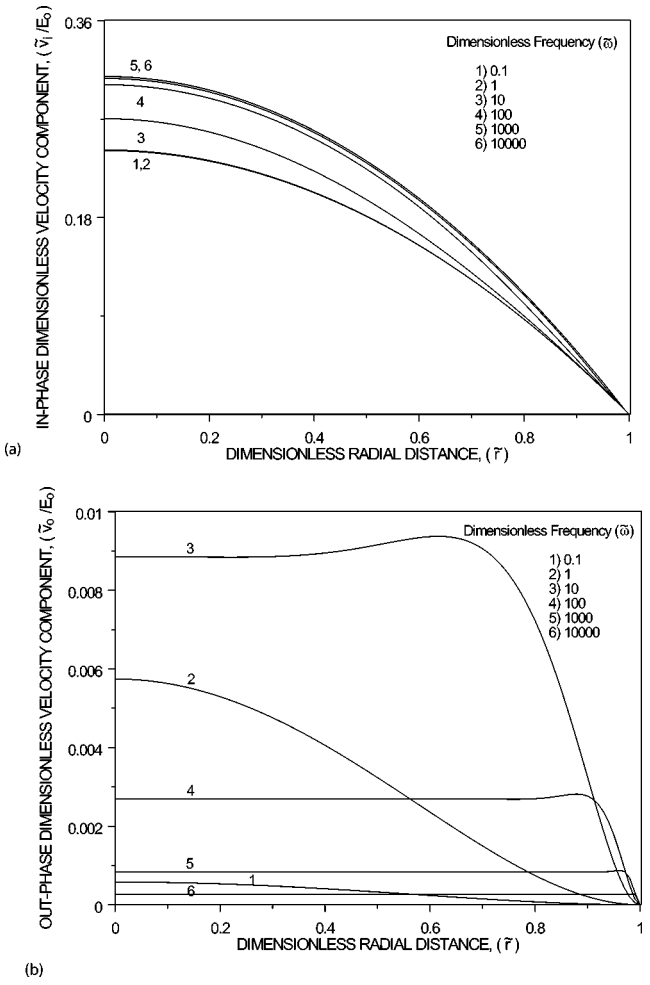

FIG. 3. Dimensionless velocity components as a function of the dimensionless radial distance ($\tilde{r}$) for dimensionless frequencies ($\tilde{\omega}$): 0.1, 1, 10, 100, 1000, and 10 000, temperature 34 °C and reactive parameter 0.2725: (a) in-phase velocity component ($\tilde{v}_i/E_o$); (b) out-phase velocity component ($\tilde{v}_o/E_o$).

ior mentioned above. Equations (35a)–(35d) establish a one-to-one correspondence between $\tilde{G}''=\tilde{G}''(T,\tilde{\omega})$ and $\tilde{G}''=\tilde{G}''(\lambda,\tilde{\omega})$.

By analyzing the dimensionless storage modulus as a function of the reactive parameter (λ) and scaled temperature (T^*) for given values of dimensionless frequency we find that this modulus is dependent of temperature and of λ as follows:

$$\lambda < 1, \quad \frac{d\tilde{G}'(\tilde{\omega})}{d\lambda} < 0 \tag{36a}$$

$$\lambda = 1, \quad \frac{d\tilde{G}'(\tilde{\omega})}{d\lambda} = 0 \tag{36b}$$

$$\lambda > 1, \quad \frac{d\tilde{G}'(\tilde{\omega})}{d\lambda} > 0 \tag{36c}$$

$$T < 38.36\ ^\circ\mathrm{C}, \quad \frac{d\tilde{G}'(\tilde{\omega})}{\mathrm{dT}} < 0 \tag{36d}$$

$$T < 38.36\ ^\circ\mathrm{C}, \quad \frac{d\tilde{G}'(\tilde{\omega})}{\mathrm{dT}} = 0, \quad \tilde{G}'(\tilde{\omega}) = 0 \tag{36e}$$

$$T > 38.36\ ^\circ\mathrm{C}, \quad \frac{d\tilde{G}'(\tilde{\omega})}{\mathrm{dT}} > 0. \tag{36f}$$

Equations (36a)–(36f) establish the one-to-one correspondence between $\tilde{G}'=\tilde{G}'(T,\tilde{\omega})$ and $\tilde{G}'=\tilde{G}'(\lambda,\tilde{\omega})$. From Eqs. (30a), (31), and (32) it follows that the correspondence principle between the T and λ effects on the storage modulus is the factorability of the λ effects:

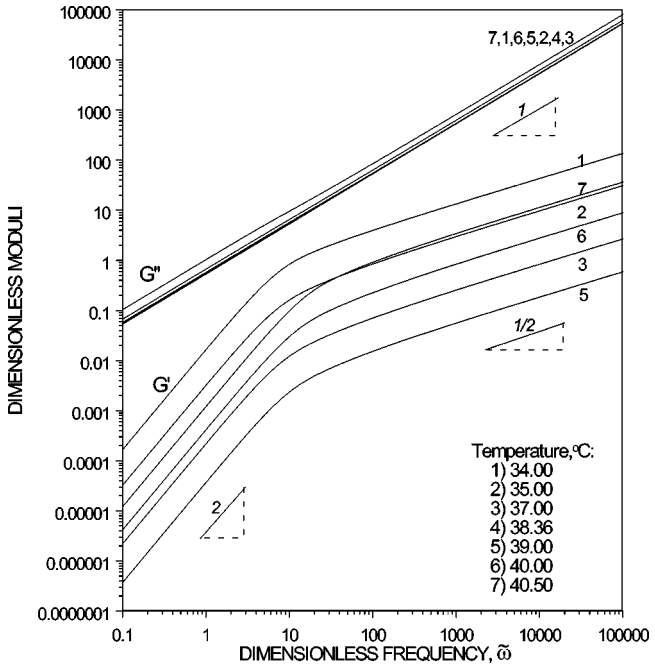

FIG. 4. Dimensionless loss modulus ($\tilde{G}''$) and dimensionless storage modulus ($\tilde{G}'$) as a function of dimensionless frequency ($\tilde{\omega}$) for temperatures 34, 35, 37, 38.36, 39, 40, and 40.5 °C. The result of G' for (4) is not shown in the plot because its value is zero for all frequencies.

$$\tilde{G}'(T,\tilde{\omega}) = g_s\left(\frac{\lambda(T)-1}{\lambda(T)+1}\right) f_s(\tilde{\omega}, M_i(T)), \tag{37}$$

where $M_i(T)$ are viscoelastic parameters. According to Eqs. (30a), (31) and (32) the storage modulus is proportional to $\tilde{\alpha}_3^2$ [and hence $(\lambda-1)^2/(\lambda+1)^2$], hence explaining the curvature of the storage modulus as a function of the reactive parameter (λ) and scaled temperature (T^*) for given values of dimensionless frequency. Using Eq. (30a) it is found that in the terminal zone, the storage modulus $\tilde{G}'$ is given by

$$\lim_{\tilde{\omega}\to o}\tilde{G}' = \lim_{\tilde{\omega}\to o}\frac{\pi E_0}{8}\frac{\tilde{\omega}\tilde{Q}_o}{(\tilde{Q}_i^{\,2}+\tilde{Q}_o^{\,2})} \propto \left(\frac{1-\lambda}{1+\lambda}\right)^2\tilde{\omega}^2 \tag{38}$$

and hence the curvature in the terminal zone is an increasing function of $\tilde{\omega}^2$: $\partial^2\tilde{G}'/\partial\lambda^2 = f(\tilde{\omega}^2)$, and for $\tilde{\omega}^2 \ll 1$ the curvature is small. On the other hand, at large frequencies

$$\lim_{\tilde{\omega}\to\infty}\tilde{G}' = \lim_{\tilde{\omega}\to\infty}\frac{\pi E_0}{8}\frac{\tilde{\omega}\tilde{Q}_o}{(\tilde{Q}_i^{\,2}+\tilde{Q}_o^{\,2})} \propto \left(\frac{1-\lambda}{1+\lambda}\right)^2\sqrt{\tilde{\omega}} \tag{39}$$

and hence for $\sqrt{\tilde{\omega}} \gg 1$ the curvature is large.

Figure 5 shows the loss angle $[\delta = \tan^{-1}(\tilde{G}''/\tilde{G}')]$ as a function of the dimensionless frequency ($\tilde{\omega}$) for T(°C): 34, 35, 37, 38.36, 39, 40, and 40.5. At the alignment-nonalignment transition ($T_{a\text{-}na} = 38.36$ °C) the storage modulus vanishes, $\delta = \pi/2$, and the material is Newtonian. The material behavior of 8CB in this flow configuration $[\mathbf{n}_0 = (0,0,1)]$ exhibits viscoelastic re-entrant behavior:

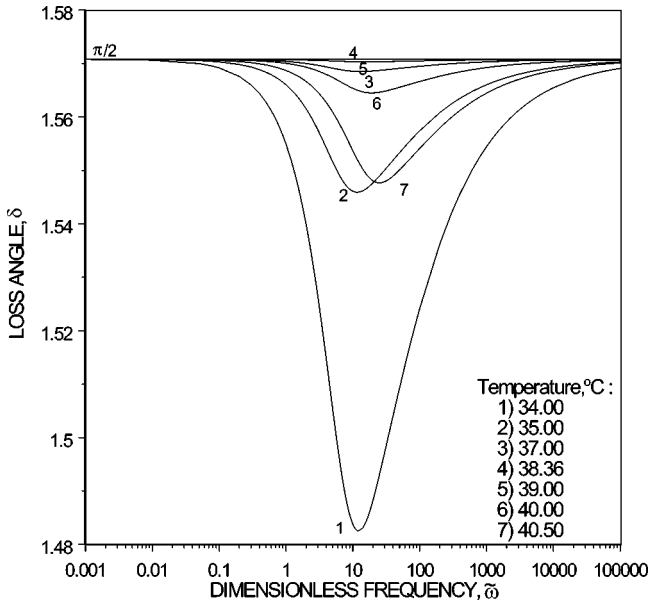

FIG. 5. Loss angle $[\delta = \tan^{-1}(\tilde{G}''/\tilde{G}')]$ as a function of the dimensionless frequency ($\tilde{\omega}$) for temperatures 34, 35, 37, 38.36, 39, 40, and 40.5 °C. The resonant behavior is classic of nematic liquid crystals [11–14].

$$\text{viscoleastic}(T < 38.36\ ^\circ\text{C}) \Rightarrow \text{purely viscous}(T = 38.36\ ^\circ\text{C}) \Rightarrow \text{viscoleastic}(T > 38.36\ ^\circ\text{C}).$$

The minimum value of the loss angle, $\min(\delta) = \delta_r$, occurs at the resonance frequency $\tilde{\omega} = \tilde{\omega}_r$ and both are functions of λ and temperature. The correspondence principle between T and λ follows from Eq. (37).

V. ASSESSING FLOW ALIGNMENT THROUGH LINEAR VISCOELASTICITY

Assessing flow alignment through linear viscoelasticity is based on the temperature dependence of the reactive parameter and the factorability principle in nematodynamics. For nematics, such as 8CB, the temperature dependence of λ in conjunction with factorability in the storage modulus gives

$$\lambda = \lambda(T), \quad \lambda(T_{a\text{-}na}) = 1, \quad \frac{d\lambda}{dT} > 1, \tag{40}$$

$$\tilde{G}'(T,\tilde{\omega}) = g_s\left(\frac{\lambda(T)-1}{\lambda(T)+1}\right) f_s(\tilde{\omega}, M_i(T));$$

$$g_s(0) = 0; \quad \text{sgn}\left(\frac{\partial\tilde{G}'}{\partial T}\right) = \text{sgn}\left(\frac{\partial\tilde{G}'}{\partial\lambda}\right), \tag{41}$$

$$\tilde{G}''(T,\tilde{\omega}) = f_1(\tilde{\omega}, \lambda(T), M_i(T)); \ \frac{\partial\tilde{G}''}{\partial T} \ll 1;$$

$$\frac{\partial\tilde{G}''}{\partial\lambda} \ll 1; \ \text{sgn}\left(\frac{\partial\tilde{G}''}{\partial T}\right) = \text{sgn}\left(\frac{\partial\tilde{G}''}{\partial\lambda}\right), \tag{42}$$

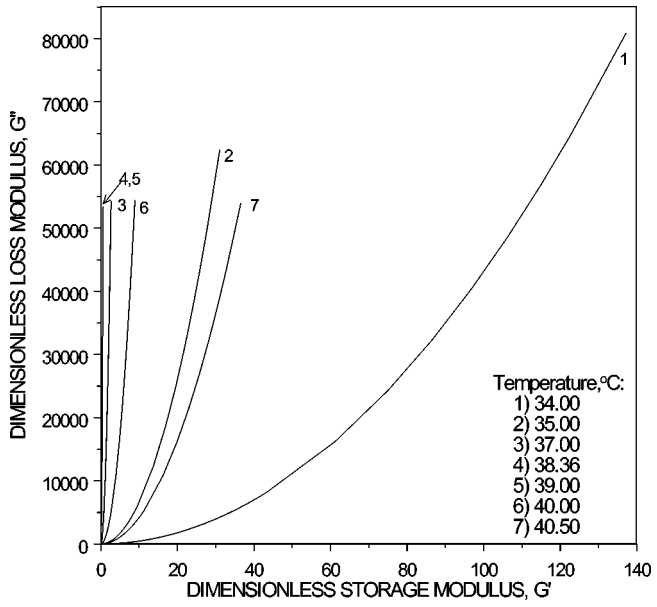

FIG. 6. Dimensionless loss modulus ($\tilde{G}''$) as a function of the dimensionless storage modulus ($\tilde{G}'$) for temperatures 34, 35, 37, 38.36, 39, 40, and 40.5 °C. Note that the slope diverges as the *A-NA* transition is approached.

$$\delta(T,\tilde{\omega}) = \tan^{-1}\left\{\frac{f_{1s}(\tilde{\omega},M_i(T))}{g_s\left(\dfrac{\lambda(T)-1}{\lambda(T)+1}\right)}\right\};$$

$$\delta(T_{a\text{-}na},\tilde{\omega}) = \tan^{-1}\left\{\frac{f_{1s}(\tilde{\omega},M_i(T))}{g_s(0)}\right\} = \frac{\pi}{2} \qquad (43)$$

and hence performing experiments at several temperatures gives unequivocal information on whether λ is greater or less than 1.

Since the alignment-nonalignment transition is reflected in the viscoelasticity as a re-entrant viscoelastic transition, we propose to capture information on flow alignment through

(i) $\tilde{G}' = f(\tilde{G}'')$,
(ii) $\delta_r = \delta_r(T)$,
(iii) $\tilde{\omega}_r = \tilde{\omega}_r(T)$.

Figure 6 shows the dimensionless loss modulus ($\tilde{G}''$) as a function of the dimensionless storage modulus ($\tilde{G}'$) for T(°C): 34, 35, 37, 38.36, 39, 40, and 40.5. The figure shows the following signatures:

(i) nonaligning regime, $T < T_{a\text{-}na}$:

$$\frac{\partial}{\partial T}\left(\frac{\partial \tilde{G}''}{\partial \tilde{G}'}\right) > 0,$$

(ii) Newtonian transition, $T = T_{a\text{-}na}$:

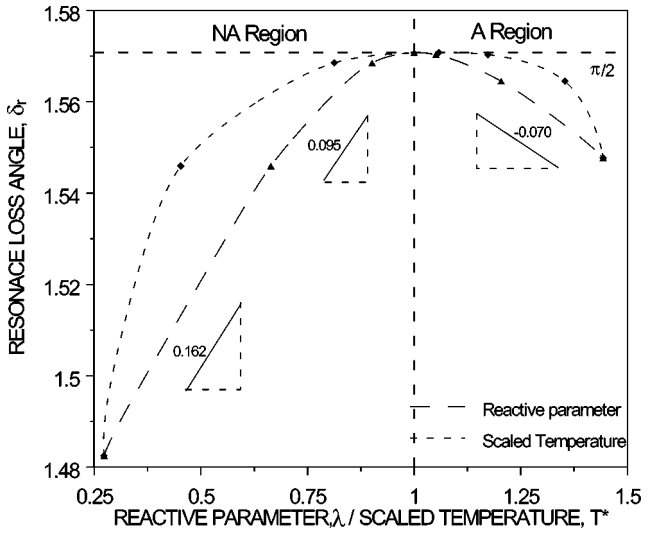

FIG. 7. Resonance loss angle (δ_r) as a function of the reactive parameter (λ) and scaled temperature (T^*), for the alignment (A) and nonalignment (NA) regions. At the *A-NA* transition the resonance loss angle is a maximum. The slope of the $d\delta_r/\mathrm{dT}$ indicates whether ($\lambda > 1$) or not.

$$\left(\frac{\partial \tilde{G}''}{\partial \tilde{G}'}\right) \to \infty,$$

(iii) aligning regime, $T > T_{a\text{-}na}$:

$$\frac{\partial}{\partial T}\left(\frac{\partial \tilde{G}''}{\partial \tilde{G}'}\right) < 0.$$

Measuring the sign of $\partial\tilde{G}''/\partial\tilde{G}'(T)$ establishes whether the material is of the aligning type or not.

Figure 7 shows the resonance loss angle (δ_r) as a function of the reactive parameter (λ), and of the scaled temperature (T^*), in the alignment and nonalignment regions. Both curves lack mirror symmetry around the *A-NA* transition. The figures show the following signatures:

(iv) nonaligning regime, $T < T_{a\text{-}na}$:

$$\frac{\partial \delta_r}{\partial T} > 0,$$

(v) Newtonian transition, $T = T_{a\text{-}na}$:

$$\delta_r = \pi/2,$$

(vi) aligning regime, $T > T_{a\text{-}na}$:

$$\frac{\partial \delta_r}{\partial T} < 0.$$

Measuring $\delta_r(T)$ establishes whether the material is of the aligning type or not.

Figure 8 shows the resonance dimensionless frequency ($\tilde{\omega}_r$) as a function of the reactive parameter (λ), and scaled temperature (T^*). The curves show the following signatures:

(i) nonaligning regime, $T < T_{a\text{-}na}$:

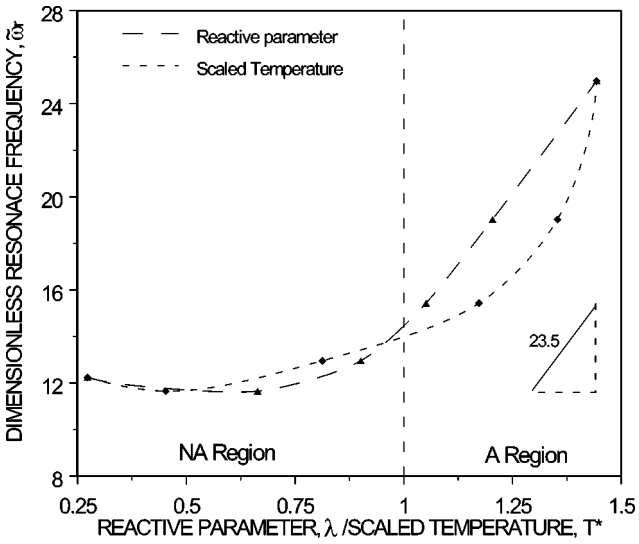

FIG. 8. Resonance dimensionless frequency ($\tilde{\omega}_r$) as a function of the reactive parameter (λ) and scaled temperature (T^*), for the alignment (A) and nonalignment (NA) regions. Note the weak slope in the NA region and the relatively large slope in the A region.

$$\text{as } T\uparrow,\ \frac{\partial\tilde{\omega}_r}{\partial T}\approx 0\rightarrow 0<\frac{\partial\tilde{\omega}_r}{\partial T}<\varepsilon,$$

(ii) aligning regime, $T>T_{a\text{-}na}$:

$$\frac{\partial\tilde{\omega}_r}{\partial T}>\varepsilon.$$

Increasing T in the nonaligning region results in a change in the slope of $\partial\tilde{\omega}_r/\partial T$. Increasing T in the aligning region increases the positive slope of $\partial\tilde{\omega}_r/\partial T$. Hence measuring $\tilde{\omega}_r(T)$ establishes whether the material is of the aligning type or not.

VI. CONCLUSIONS

The Leslie-Ericksen equations for small-amplitude oscillatory Poiseuille flow of 8CB (4-n-octyl-4′-cyanobiphenyl) were solved using analytical and scaling methods. This SMRNLC is flow aligning for $T>38.36\ ^\circ$C and nonaligning for $T<38.36\ ^\circ$C. The storage G' and loss G'' modulus are those of a viscoelastic material with a single relaxation time, such that the loss angle δ exhibits a resonance peak at a frequency ω_r. The dependence of linear viscoelastic material functions on temperature and reactive parameter were established. It was found that the aligning-nonaligning transition is a reentrant viscoelastic transition and that when the director is aligned along the flow direction the behavior is purely Newtonian when $\lambda=1$.

It is shown that since the major temperature effects on the storage modulus G' are through a factorable function of the reactive parameter: $G'(T,\omega,M)=g[\lambda(T)]f(\omega,M)$, flow alignment in nematic liquid crystals can be determined using the temperature dependence of the linear viscoleastic response to small-amplitude oscillations. In particular measuring $\partial\tilde{G}''/\partial\tilde{G}'(T)$, $\delta_r(T)$, $\omega_r(T)$ provides unequivocal evidence on whether the nematic liquid crystal is of the aligning or nonaligning type. Since linear viscoelasticity is a simple and easily accessible measurement, the proposed methodology is a helpful and economical tool for nematodynamicists.

ACKNOWLEDGMENTS

This research was supported by the Engineering Research Centers Program of the National Science Foundation under NSF Award No. EEC-9731680. One of us (L.R.P.d.A.L.) also gratefully acknowledges the support of the Natural Sciences and Engineering Research Council of Canada (NSERC).

[1] F. R. S. Chandrasekhar, *Liquid Crystals*, 2nd Ed. (Cambridge University Press, Cambridge, England, 1992).
[2] P. G. de Gennes, and J. Prost, *The Physics of Liquid Crystals*, 2nd Ed. (Oxford University Press, London, 1993).
[3] W. H. Han and A. D. Rey, J. Rheol. **39**, 301 (1995).
[4] A. D. Rey and M. M. Denn, Annu. Rev. Fluid Mech. **34**, 233 (2002).
[5] R. G. Larson, *The Structure and Rheology of Complex Fluids* (Oxford University Press, New York, 1999).
[6] J. K. Moscicki, in *Physical Properties of Liquid Crystals: Nematics*, edited by D. A. Dunmur, A. Fukuda, and G. Luckhurst (IEE Publishing, London, 2001), pp. 387–404.
[7] H. A. Barnes, J. F. Hutton, and K. Walters, *An Introduction to Rheology* (Elsevier Science, New York, 1989).
[8] R. B. Bird, R. C. Armstrong, and O. Hassager, *Dynamics of Polymeric Liquids* (John Wiley & Sons, New York, 1989).
[9] S. V. Pasechnik, V. A. Tsvetkov, A. V. Torchinskaya, and D. O. Karandashov, Mol. Cryst. Liq. Cryst. Sci. Technol., Sect. A, Sect. A **366**, 165 (2001).
[10] S. A. Pikin, *Structural Transformations in Liquid Crystals* (Gordon and Breach, New York, 1991).
[11] W. R. Burghardt, J. Rheol. **35**, 49 (1991).
[12] A. D. Rey, Mol. Cryst. Liq. Cryst. Sci. Technol., Sect. A, Sect. A **281**, 155 (1996).
[13] A. D. Rey, J. Rheol. **44**, 855 (2000).
[14] A. D. Rey, J. Rheol. **46**, 225 (2002).
[15] L. Ramos, M. Zapotocky, T. C. Lubensky, and D. A. Weitz, Phys. Rev. E **66**, 031711 (2002).
[16] M. Yada, J. Yamamoto, and H. Yokoyama, Langmuir **19**, 3650 (2003).
[17] J. L. Ericksen, Trans. Soc. Rheol. **5**, 23 (1961).
[18] F. M. Leslie, Arch. Ration. Mech. Anal. **28**, 265 (1968).
[19] F. M. Leslie, Adv. Liq. Cryst. **4**, 1 (1979).
[20] L. R. P. de Andrade Lima and A. D. Rey, J. Rheol. **47**, 1261 (2003).
[21] M. B. Lacerda Santos, Y. Galerne, and G. Durand, J. Phys. (Paris) **46**, 933 (1985).
[22] H. Kneppe, F. Schneider, and N. K. Sharma, Ber. Bunsenges.

Phys. Chem. **85**, 784 (1981).
[23] H. Kneppe, F. Schneider, and N. K. Sharma, J. Chem. Phys. **77**, 3203 (1982).
[24] M. Abramowitz and I. A. Stegun, *Handbook of Mathematical Functions* (Dover Publications, New York, 1972).
[25] A. D. Rey and M. M. Denn, J. Non-Newtonian Fluid Mech. **27**, 375 (1988).
[26] L. R. P. de Andrade Lima and A. D. Rey, J. Non-Newtonian Fluid Mech. **110**, 103 (2003).